# DNA-Induced Aggregation of Zwitterionic Oligolamellar Liposome

Ching-Mao Wu,[†] Hsin-Lung Chen,*[,†] Willisa Liou,[‡] Tsang-Lang Lin,[§] and U-Ser Jeng[||]

*Department of Chemical Engineering and Department of Engineering and System Science, National Tsing Hua University, Hsin-Chu, Taiwan 30013, Republic of China, Department of Anatomy, Chang Gung University, Kwei-San, Taoyuan 333, Taiwan, Republic of China, and National Synchrotron Radiation Research Center, Hsin-Chu, Taiwan 300, Republic of China*

*Received August 10, 2004*

Liposome consisting of a single zwitterionic lipid as the potential vector for gene therapy has been reported recently; however, whether polyanionic DNA can bind directly with zwitterionic lipid without the aid of multivalent salt still remains unresolved. In this study, we reveal the aggregation of zwitterionic oligolamellar liposomes composed of 1,2-di(*cis*-9-octadecenoyl)-*sn*-glycero-3-phosphocholine induced by DNA without the presence of multivalent salt. Our results demonstrate that only a small fraction (<10%) of DNA can bind electrostatically with a portion of the liposomes. Such a low degree of binding, however, induces significant aggregation of these oligolamellar liposomes, yielding large multilamellar particles in which the number of hydrophilic/hydrophobic layer stacking becomes sufficiently large to yield multiple diffraction peaks in the small-angle X-ray scattering profile. Addition of monovalent salt such as NaCl tends to disrupt the multilamellar structure.

## Introduction

Over the past decade, much attention has been directed to the complexes of DNA with cationic liposomes (CLs) because of their potential application as a nonviral vector for gene therapy.[1−3] What remains to be clarified to date is the mechanism of CL-mediated nucleic acid delivery, where characterizing the self-assembled structures of DNA/CL complexes is crucial to build the detailed mechanism.

The complexation between polyanionic DNA and CL is driven by their spontaneous electrostatic interaction coupled with the entropic gain from counterion release. Experimental observations based on X-ray scattering and microscopy have revealed that the complexation induced a topological transformation of the CL where uni- or oligolamellar vesicles aggregated and fused into condensed particles.[4−24] Two types of condensed phase have been observed; the predominant one was a multilamellar phase with DNA intercalating between the lipid bilayers forming arrays of in-plane smectic orders (denoted by "$L_\alpha{}^C$" phase),[4,5] and the other was an inverted hexagonal phase consisting of DNA encapsulated into hexagonally arranged lipid tubes (denoted by "$H_{II}{}^C$" phase).[6]

It is noted that the CL used as a gene vector is commonly a mixture of a synthetic cationic lipid (cytofectin) and a neutral zwitterionic lipid (ZL; also called "helper lipid").[2] The ZL is added to reduce the cytotoxicity and to enhance the compatibility with the cell membrane. In this sense, use of a single ZL component to encapsulate DNA would be an advantageous approach for gene therapy. This idea has been put forth recently by Pott and Roux who investigated a DNA/ZL system prepared by mixing DNA with a ZL, 1,2-di(*cis*-9-octadecenoyl)-*sn*-glycero-3-phosphocholine (DOPC), in water followed by freeze-drying and finally rehydration of the mixture to the water content of 50%.[25] The resultant DNA/DOPC mixture was found to exhibit an ordered multilamellar structure, in which the DNA sandwiched between the bilayers arranged in an in-plane smectic order,[25] such as that found in DNA/CL complexes. The results appear to imply that a favorable binding between DNA and ZL exists despite the charge neutrality of the ZL molecule. DNA−ZL binding has also been purported in other studies. Using UV−vis spectroscopy, Monnard et al. demonstrated the entrapment of DNA in the ZL membrane though the extent of entrapment was fairly low.[26] Malghani and Yang had observed the adsorption of DNA on the zwitterionic dipalmitoylphosphatidylcholine (DPPC) bilayer film in an aqueous NaCl solution using atomic force microscopy (AFM).[27]

Despite these experimental findings, several studies have suggested that DNA hardly bound to ZL unless divalent or multilvalent cations were added.[28−32] These cations bound with DNA on one side and with the anionic moiety in the ZL on the other and, hence, served as the bridge between them.[28−32] In this case, the DNA/ZL system behaved like a DNA/CL complex, where the transformation of the liposome structure into a condensed multilamellar phase in which the DNA chains formed smectic arrays may occur.

In the present study, we revisit the problem of DNA−ZL binding in the absence of multivalent cation by resolving

* To whom correspondence should be addressed.
[†] Department of Chemical Engineering, National Tsing Hua University.
[‡] Chang Gung University.
[§] Department of Engineering and System Science, National Tsing Hua University.
[||] National Synchrotron Radiation Research Center.

10.1021/bm0495396 CCC: $27.50 © 2004 American Chemical Society
Published on Web 10/05/2004

both the structure of the DNA/DOPC mixture using small-angle X-ray scattering (SAXS) and transmission electron microscopy (TEM) and the amount of DNA bound to DOPC liposome using UV−vis spectroscopy. It will be shown that a small fraction of DNA can indeed bind electrostatically with the DOPC liposome. The low degree of binding induces significant aggregation of the originally oligolamellar liposomes, yielding large multilamellar particles. It should be noted that the present study is distinguished from the previous study of the DNA/DOPC system (with a lower water content) prepared by rehydrating the freeze-dried mixture,[25] in that we are dealing with the system as prepared in a large excess amount of pure water without subjecting it to any post-drying/rehydration treatment.

## Experimental Section

**Materials and Liposome Preparation.** DOPC was obtained from Sigma in the lyophilized powder and was used directly without further purification. Linear DNA from herring testes was also acquired from Sigma in the form of sodium salt. The size of DNA determined by gel electrophoresis had a center of distribution at about 700 bps.[33] All the water used in the present work was distilled and purified using a Milli-Q plus instrument from Millipore. The quality of the water was characterized by a conductivity of 18.5 ± 0.1 MΩ cm and a pH of 6.7 ± 0.2 (∼20 °C).

For the preparation of the oligolamellar DOPC liposomes, the appropriate amount of DOPC was dissolved in freshly distilled chloroform. The solution was directly dried under vacuum for 3 h to completely remove the solvent. The resulting lipid film was hydrated by deionized water for 30 min at room temperature and another 10 min of mixing by a vortex mixer. The size reduction of the vesicles was carried out by sonication in a temperature-controlled ultrasonic bath at 40 °C, after which the suspension with a vesicle size between 400 and 200 nm in diameter as measured by dynamic light scattering (DLS-700, Otsuka Electronics Co., Ltd.) was obtained. The DNA/DOPC suspension was prepared by rapidly mixing DNA (10 mg/mL) with the DOPC suspension at the desired compositions. This mixing resulted in visually observable precipitation. The overall composition of the mixture was expressed by the lipid-to-base-pair molar ratio ($\nu$). The concentration of DNA/DOPC in water was controlled at around 5.0 wt % (or water content ≈95 wt %).

**SAXS Measurements.** The specimens for SAXS measurement were prepared by directly introducing the aqueous suspension into the sample cell comprising two Kapton windows. The in-house SAXS apparatus consisted of an 18 kW rotating anode X-ray generator (Rigaku) operated at 200 mA and 40 kV, a pyrotic graphite crystal for incident beam monochromatization, and a two-dimensional position-sensitive detector (ORDELA model 2201X, Oak Ridge Detector Laboratory, Inc., U.S.A.) with 256 × 256 channels (active area 20 × 20 cm$^2$ with ∼1-mm resolution). The SAXS measurement was conducted at 20 °C with the data acquisition time of 1 h for each sample. The sample remained stable after the X-ray exposure. As a matter of fact, the SAXS profile obtained by 5 h of exposure was identical to that collected with 1 h of counting time, indicating that the structure of the system was not damaged during the SAXS measurement.

All the SAXS data had been corrected for the background (dark current and empty beam scattering) and the sensitivity of each pixel of the area detector. The area scattering pattern had been radially averaged to increase the efficiency of data collection. The resulting intensity profile was output as a plot of the scattering intensity ($I$) versus the scattering vector, $q = (4\pi/\lambda)\sin(\theta/2)$ ($\theta$ = scattering angle). All the intensity profiles reported here had also been corrected for the thermal diffuse scattering (TDS). TDS was considered as a positive deviation from Porod's law and might be associated with thermal motion, local disorder, or onset of the wide-angle scattering region. The intensity level of TDS was assumed to be a constant, and its magnitude was determined from the slope of the $Iq^4$ versus $q^4$ plot at the high-$q$ region.[34]

**TEM Observations.** The TEM specimens of DOPC liposomes and DNA/DOPC precipitates were prepared by a negative staining method which effectively vitrified the structure in the excess water state.[35] A 5-$\mu$L drop of the aqueous suspension was deposited onto a copper grid bearing a carbon-coated Formvar film. The solution was allowed to stand for 1 min and was then withdrawn with the tip of a piece of filter paper until a very thin layer of fluid formed on the grid surface. The samples were immediately stained for 1 min with an aqueous 4% acidic uranyl acetate solution and 1 min in a methycellulose/uranyl acetate mixture (1.8/0.3%). The ultrathin specimens were then examined by a JEOL 2000EXII transmission electron microscope operated at 100 kV.

**UV−Vis Spectroscopy Experiment.** UV−vis spectroscopy (Hitachi U-3300 spectrophotometer) was employed to determine the amount of DNA bound with the DOPC liposomes (in the precipitate) by measuring the concentration of free DNA remaining in the supernatant from the absorbance of the DNA peak near 260 nm.

## Results and Discussion

We first examine the structure of neat DOPC liposomes prepared according to the procedure described in the Experimental Section. Figure 1 shows the Lorentz-corrected SAXS profile of the liposomes. The scattering pattern is characterized by a broad diffuse halo, indicating that the liposomes do not exhibit an ordered multilamellar structure. The representative TEM micrograph of the liposomes is displayed in Figure 2. Oligolamellar vesicles (consisting of 3−8 hydrophilic/hydrophobic layers per vesicle) with the dark and gray striations corresponding to the hydrophilic and hydrophobic layers, respectively, are predominantly observed. In this case, the average number of lamellar stacks within individual liposomes is too few to yield multiple diffraction peaks in the corresponding SAXS profile. It should be noted that multiple diffraction peaks characteristic to multilamellar structure had indeed been observed in the previous studies of similar zwitterionic liposomes at an even higher water content. This is because the liposomes studied therein were multilamellar vesicles prepared without additional sonication after hydrating the dry lipid film. In the present study, however, the sonication was applied to produce

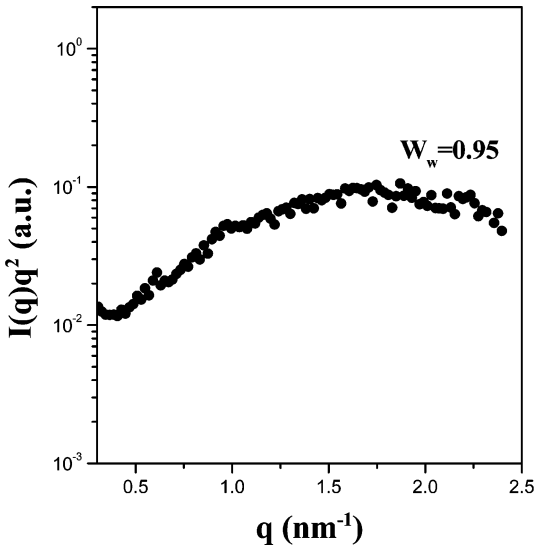


**Figure 1.** Lorentz-corrected SAXS profile of neat DOPC liposomes. The scattering pattern is characterized by a broad diffuse halo, indicating that the liposomes do not exhibit an ordered multilamellar structure.

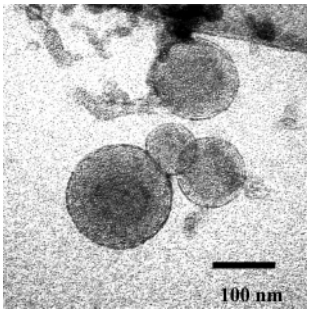


**Figure 2.** Representative TEM micrograph of neat DOPC liposomes. Oligolamellar vesicles (consisting of 3−8 hydrophilic/hydrophobic layers per vesicle) with the dark and gray striations corresponding to the hydrophilic and hydrophobic layers, respectively, are predominantly observed.

oligolamellar vesicles because of our interest in revealing whether DNA may bind with the oligolamellar liposomes and subsequently induces aggregation and topological transformation of these liposomes.

The binding of DNA with DOPC liposomes is indeed manifested by the visually observable precipitation upon adding DNA into the DOPC liposome suspension, as demonstrated in Figure 3 showing the photographs of neat DOPC and DNA/DOPC ($\nu = 2.0$) suspensions. Precipitate of DNA/DOPC (indicated by the arrow) is clearly observed at the bottom of the container, indicating aggregation of the oligolamellar liposomes to form large particles upon binding with DNA. The degree of binding is, however, not 100% as the cloudy supernatant signals the presence of unbound DOPC liposomes.

Likewise, the DNA added into the system may not fully bind with DOPC liposomes even when DOPC is in excess of DNA in terms of the molar ratio (i.e., $\nu > 2.0$). We define the binding ratio of DNA as

$$\text{binding ratio (\%)} = \frac{C_{\text{DNA}}{}^{0} - C_{\text{DNA}}{}^{\text{s}}}{C_{\text{DNA}}{}^{0}} \times 100 \qquad (1)$$

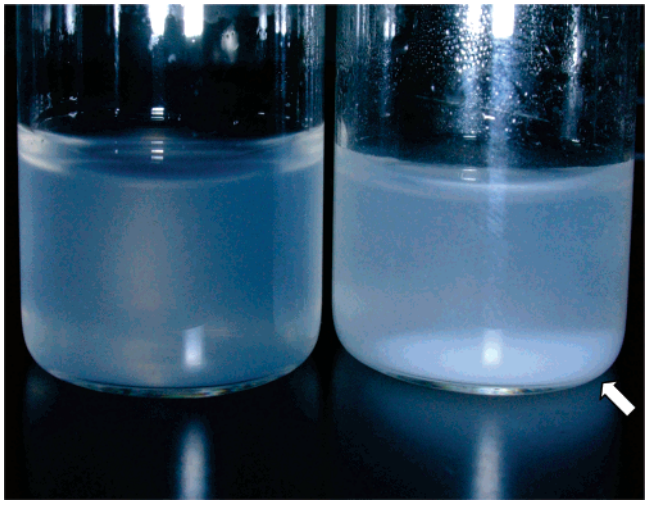

**Figure 3.** Photographs showing the appearances of neat DOPC (left) and DNA/DOPC ($\nu = 2.0$) suspensions. Precipitate of DNA/DOPC (indicated by the arrow) is clearly observed at the bottom of the container, indicating aggregation of the oligolamellar liposomes into large particles upon binding with DNA.

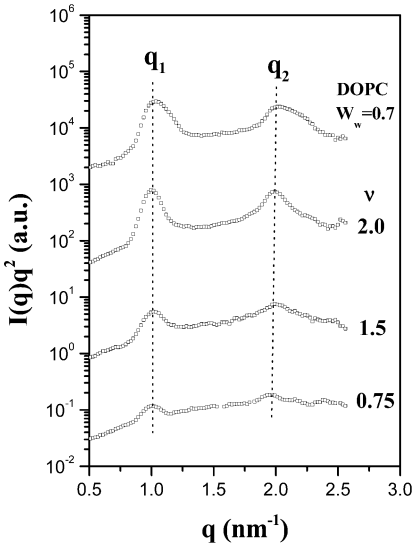


**Figure 4.** Lorentz-corrected SAXS profiles showing two diffraction peaks for the DNA/DOPC precipitates in the samples with various overall lipid-to-base-pair molar ratios. Also shown here is the SAXS profile of multilamellar DOPC liposomes prepared without imposing sonication to the liposome suspension. It can be seen that the SAXS patterns of the DNA/DOPC precipitates and of neat DOPC liposomes are essentially the same in terms of the positions and relative intensities of the scattering peaks.

where $C_{\text{DNA}}{}^{0}$ is the total concentration of DNA and $C_{\text{DNA}}{}^{\text{s}}$ is the concentration of free DNA remaining in the supernatant. $C_{\text{DNA}}{}^{\text{s}}$ can be determined from the absorbance of the peak at 260 nm in the UV−vis spectrum of the supernatant. The result indicates that the binding ratio is only about 9% irrespective of the overall lipid-to-base-pair molar ratio. Without the aid of multivalent cations (e.g., $Ca^{2+}$), therefore, only a small amount of DNA can bind with the DOPC liposomes. Free DNA, unbound DOPC oligolamellar vesicles, and the DNA/DOPC precipitates, thus, coexist in the system irrespective of the overall lipid-to-base-pair molar ratio.

We now proceed to examine the structure of the precipitate containing DNA-bound DOPC. Figure 4 shows the Lorentz-corrected SAXS profiles obtained from the precipitates in

the samples with various overall lipid-to-base-pair molar ratios. In contrast to the scattering pattern of neat DOPC, two equally spaced peaks are observed at $q_1 = 1.00$ nm$^{-1}$ and $q_2 = 1.98$ nm$^{-1}$ irrespective of $\nu$. This demonstrates the formation of a multilamellar phase with the interlamellar distance $d = 2\pi/q_1 = 6.3$ nm in the precipitates. On basis of the UV−vis and SAXS results, it can, hence, be inferred that a small fraction of DNA can bind directly with zwitterionic DOPC liposomes without the aid of multivalent cations. This low degree of binding induces aggregation of the oligolamellar liposomes into large multilamellar particles (precipitates) in which the number of hydrophilic/hydrophobic layers along the lamellar stacking direction becomes sufficiently large to yield multiple diffraction peaks in the SAXS profile.

It should be noted that liposome aggregation and transformation of the SAXS pattern from a broad halo into multilamllar diffraction peaks upon adding DNA have also been observed in the complexation between DNA and CL.[36] This, however, does not necessarily mean that the binding and self-assembly behavior of the DNA/ZL system is identical or even similar to that of DNA/CL complexes. In DNA/CL complexes, intercalation of polyanionic DNA chains is found in all hydrophilic layers due to their strong electrostatic interaction with the cationic membrane surface. The prevalent DNA intercalation may be manifested by the shift of interlamellar distance (relative to that of neat CL) and the emergence of a new peak in the electron density profile of the hydrophilic region obtained from the relative intensities of the diffraction peaks.[25,36] The DNA chains confined in the hydrophilic layers also tend to organize into a smectic order that gives rise to a DNA−DNA correlation peak in the corresponding SAXS profile.

To reveal whether DNA is intercalated prevalently in the hydrophilic layers, we compare the SAXS profiles of the DNA/DOPC precipitates with that of multilamellar DOPC liposomes prepared without imposing sonication on the liposome suspension, as shown in Figure 4. It can be seen that the SAXS patterns of these two systems are essentially the same in terms of the positions and relative intensities of the scattering peaks, signaling that both the interlamellar distance and the electron density profile along the lamellar normal (governed by the relative peak intensities) associated with the corresponding multilamellar phases are virtually identical. Therefore, in contrast to DNA/CL complexes, most hydrophilic layers in the DNA/DOPC precipitate particles are DNA-free. The binding of DNA with the oligolamellar DOPC liposomes must then predominantly occur at the surface of the vesicles, where binding of one side of the DNA chain to a vesicle and the other side to another vesicle results in liposome aggregation. In the resultant precipitate particles, the DNA chains are located at the boundary between the liposomes and the sequential stacking of hydrophilic and hydrophobic layers across the boundary gives rise to multilamellar diffraction peaks. This morphological picture is confirmed by the TEM observation in Figure 5. It can be seen that the DNA/DOPC precipitate particles are simply formed by the aggregation of a number of oligolamellar liposomes, while these liposomes did not fuse and reorganize further to form the compact multilamellar particles found in the DNA/CL complexes.

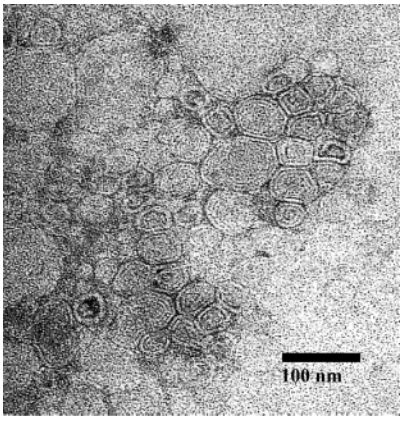


**Figure 5.** Representative TEM micrograph showing the morphology of the DNA/DOPC precipitate particles. It can be seen that the particles are simply formed by the aggregation of a number of the oligolamellar DOPC liposomes, while these liposomes did not fuse and reorganize further to form the compact multilamellar particles found in the DNA/CL complexes.

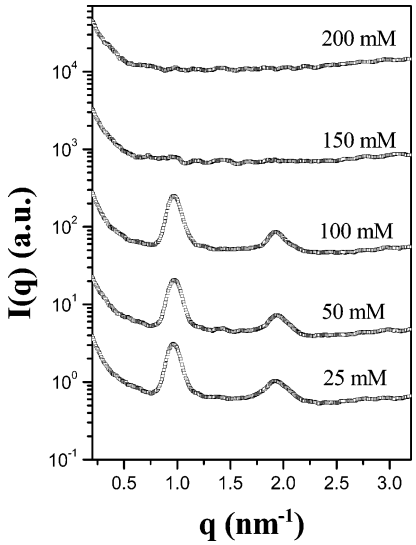


**Figure 6.** SAXS profiles of DNA/DOPC with $\nu = 2.0$ dispersed in aqueous NaCl solutions with various NaCl concentrations.

In addition to the lack of prevalent DNA intercalation, no additional peak associated with the in-plane correlation of the DNA chains located at the boundary between the liposomes is observed in the SAXS profiles. Considering that the binding ratio of DNA is fairly low, the DNA−DNA correlation peak may be too weak to be resolved in the SAXS profile. Moreover, according to the AFM investigation by Malghani and Yang,[27] the DNA chains adsorbed on the supported zwitterionic DPPC bilayers were found to arrange in a rather isotropic way instead of a fairly ordered smectic array as a result of the low degree of adsorption. In this sense, we may expect the in-plane correlation of the DNA chains to be too weak to yield a peak in the SAXS profile.

The results presented thus far have demonstrated that DNA has the ability to bind with zwitterionic DOPC in excess water without the aid of multivalent salts. The attractive interactions should be electrostatic in nature where the positive charge at the headgroup of DOPC interacts attractively with the negative charge on DNA. To testify this

postulate, we add a univalent NaCl salt into the DNA/DOPC mixture to see if the salt is able to screen the electrostatic interaction and, hence, disrupts the multilamellar structure formed by the liposome aggregation. Figure 6 shows a series of SAXS profiles of DNA/DOPC with $\nu = 2.0$ subjected to exposure of various NaCl concentrations in aqueous solution. The lamellar order still remains when the NaCl concentration lies below 100 mM; however, when the concentration is increased to above 150 mM the lamellar order is completely disrupted, signifying that the monovalent $Na^+$ forms a screening layer to screen the electrostatic attraction between DNA and DOPC and thereby causes DNA to demix from the DNA/DOPC aggregates.

## Conclusions

In conclusion, the present work shows that polyanionic DNA can bind electrostatically with zwitterionic DOPC lipids in an excess amount of water without the aid of multivalent cations. The low degree of binding induced significant aggregation of the oligolamellar DOPC liposomes into large multilamellar particles. The lack of prevalent intercalation of DNA in the hydrophilic layers in these particles indicated that DNA only bound to the surfaces of the liposomes. Such a surface binding resulted in liposome aggregation, where the liposomes after aggregation did not fuse or reorganize further to form the compact multilamellar particles found in DNA/CL complexes. As a result of the weak electrostatic interaction, the multilamellar structure in the DNA/DOPC particles could be easily disrupted by the addition of a monovalent salt such as NaCl.

**Acknowledgment.** This work was supported by the National Science Council of R.O.C. under Grant NSC 91-2216-E-007-016.

## References and Notes

(1) Lasic, D. D.; Templeton, N. S. *Adv. Drug Delivery Rev.* **1996**, *20*, 221−266.
(2) Miller, A. D. *Angew. Chem., Int. Ed.* **1998**, *37*, 1768−1785.
(3) Chesnoy, S.; Huang, L. *Annu. Rev. Biophys. Biomol. Struct.* **2000**, *29*, 27−47.
(4) Rädler, J. O.; Koltover, I.; Salditt, T.; Safinya, C. R. *Science* **1997**, *275*, 810−814.
(5) Lasic, D. D.; Strey, H.; Stuart, M. C. A.; Podgornik, R.; Frederik, P. M. *J. Am. Chem. Soc.* **1997**, *119*, 832−833.
(6) Koltover, I.; Salditt, T.; Rädler, J. O.; Safinya, C. R. *Science* **1998**, *281*, 78−81.
(7) Rädler, J. O.; Koltover, I.; Jamieson, A.; Salditt, T.; Safinya, C. R. *Langmuir* **1998**, *14*, 4272−4283.
(8) Sternberg, B.; Sorgi, F. L.; Huang, L. *FEBS Lett.* **1994**, *356*, 361−366.
(9) Huang, L.; Hung, M. C.; Wagner, E. *Nonviral Vectors for Gene Therapy*; Academic Press: New York, 1999.
(10) Gustafsson, J.; Arvidson, G.; Karlsson, G.; Almgren, M. *Biochim. Biophys. Acta* **1995**, *1235*, 305−312.
(11) Pitard, B.; Aguerre, O.; Airiau, M.; Lachages, A. M.; Boukhnikachvili, T.; Byk, G.; Dubertret, C.; Herviou, C.; Scherman, D.; Mayaux, J. F.; Crouzet, J. *Proc. Natl. Acad. Sci. U.S.A.* **1997**, *94*, 14412−14417.
(12) Koltover, I.; Salditt, T.; Safinya, C. R. *Biophys. J.* **1999**, *77*, 915−924.
(13) Koltover, I.; Wagner, K.; Safinya, C. R. *Proc. Natl. Acad. Sci. U.S.A.* **2000**, *97*, 14046−14051.
(14) Fang, Y.; Yang, J. *J. Phys. Chem. B* **1997**, *101*, 441−449.
(15) Fang, Y.; Yang, J. *J. Phys. Chem. B* **1997**, *101*, 3453−3456.
(16) Fang, Y.; Hoh, J. H. *J. Am. Chem. Soc.* **1998**, *120*, 8903−8909.
(17) Ono, M. Y.; Spain, E. M. *J. Am. Chem. Soc.* **1999**, *121*, 7330−7334.
(18) Leonenko, Z. V.; Merkle, D.; Lees-Miller, S. P.; Cramb, D. T. *Langmuir* **2002**, *18*, 4873−4884.
(19) Battersby, B. J.; Grimm, R.; Huebner, S.; Cevc, G. *Biochim. Biophys. Acta* **1998**, *1372*, 379−383.
(20) Huebner, S.; Battersby, B. J.; Grimm, R.; Cevc, G. *Biophys. J.* **1999**, *76*, 3158−3166.
(21) Schmutz, M.; Durand, D.; Debin, A.; Palvadeau, Y.; Etienne, A.; Thierry, A. R. *Proc. Natl. Acad. Sci. U.S.A.* **1999**, *96*, 12293−12298.
(22) Pitard, B.; Oudrhiri, N.; Vigneron, J. P.; Hauchecorne, M.; Aguerre, O.; Toury, R.; Airiau, M.; Ramasawmy, R.; Scherman, D.; Crouzet, J.; Lehn, J. M.; Lehn, P. *Proc. Natl. Acad. Sci. U.S.A.* **1999**, *96*, 2621−2626.
(23) Raspaud, E.; Pitard, B.; Durand, D.; Aguerre-Chariol, O.; Pelta, J.; Byk, G.; Scherman, D.; Livolant, F. *J. Phys. Chem. B* **2001**, *105*, 5291−5297.
(24) Zantl, R.; Baicu, L.; Artzner, F.; Sprenger, I.; Rapp, G.; Rädler, J. O. *J. Phys. Chem. B* **1999**, *103*, 10300−10310.
(25) Pott, T.; Roux, D. *FEBS Lett.* **2002**, *511*, 150−154.
(26) Monnard, P.; Berclaz, N.; Conde-Frieboes, K.; Oberholzer, T. *Langmuir* **1999**, *15*, 7504−7509.
(27) Malghani, M. S.; Yang, J. *J. Phys. Chem. B* **1998**, *102*, 8930−8933.
(28) Tarahovsky, Y. S.; Khusainova, R. S.; Gorelov, A. V.; Nicolaeva, T. I.; Deev, A. A.; Dawson, A. K.; Ivanitsky, G. R. *FEBS Lett.* **1996**, *390*, 133−136.
(29) Kharakoz, D. P.; Khusainova, R. S.; Gorelov, A. V.; Dawson, K. A. *FEBS Lett.* **1999**, *446*, 27−29.
(30) Hayes, M. E.; Gorelov, A. V.; Dawson, K. A. *Prog. Colloid Polym. Sci.* **2001**, *118*, 243−247.
(31) Francescangeli, O.; Stanic, V.; Gobbi, L.; Bruni, P.; Iacussi, M.; Tosi, G. *Phys. Rev. E* **2003**, *67*, 011904.
(32) McManus, J. J.; Rädler, J. O.; Dawson, K. A. *J. Phys. Chem. B* **2003**, *107*, 9869−9875.
(33) Dias, R.; Mel'nikov, S.; Lindman, B.; Miguel, M. G. *Langmuir* **2000**, *16*, 9577−9583.
(34) Medellin-Rodriguez, F. J.; Phillips, P. J.; Lin, J. S. *Macromolecules* **1996**, *29*, 7491−7501.
(35) Liou, W.; Geuze, H. J.; Slot, J. W. *Histochem. Cell Biol.* **1996,** *106*, 41−58.
(36) Wu, C.-M.; Liou, W.; Chen, H.-L.; Lin, T.-L.; Jeng, U.-S. *Macromolecules* **2004**, *37*, 4974−4980.

BM0495396